Preliminary Results of a 20 K X-Ray Study of Citrinin *

R. Destro and F. Merati

Dipartimento di Chimica Fisica ed Elettrochimica e Centro CNR, Università di Milano, Via Golgi 19, 20133 Milano, Italy

Z. Naturforsch. **48a**, 99–104 (1993); received October 18, 1991

A total of about 37 000 diffracted intensities has been measured at 20 K for a spherical single crystal of citrinin. Using a multipole formalism to interpret the X-ray data, maps of the charge density and of its Laplacian, as well as for the electrostatic potential have been derived. A value of 7(2) D has been obtained for the magnitude of the molecular dipole moment. A study of the electric field gradient (EFG) at the nuclei has yielded the atomic quadrupole coupling constants (QCC) and asymmetry parameters (η). A topological analysis of the charge density has been performed to characterize the intramolecular covalent and hydrogen bonds.

Key words: Electrostatic properties; Charge density; Topological analysis; Very low temperature; Citrinin.

Introduction

Citrinin is an extensively studied fungal metabolite, whose chemical structure was determined years ago by degradative, synthetic and spectroscopic techniques. Careful X-ray diffraction studies at room temperature and at 147 K have established [1] the tautomeric forms, superimposed on each other, in the crystals of this compound: at room temperature two tautomers were found in a ratio of about 3:2, the p-quinone methide tautomer predominating over the o-quinone; at 147 K only the *para* tautomer was found.

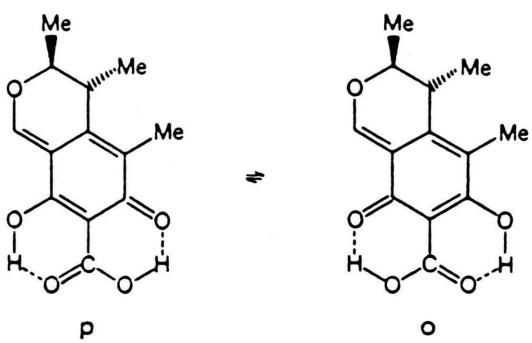

Those studies have been subsequently extended by measuring, from another crystal of the same compound, X-ray diffracted intensities at various temperatures, in the sequence: 293, 20, 240, and again 293 K. From the combined X-ray results of the two investigations, the thermodynamic parameters for the *proton transfer* occurring in the crystals of citrinin have been derived [2]. Furthermore, it has been shown that it can be safely assumed that the 20 K X-ray structure of citrinin describes the pure p-quinonemethide form. In

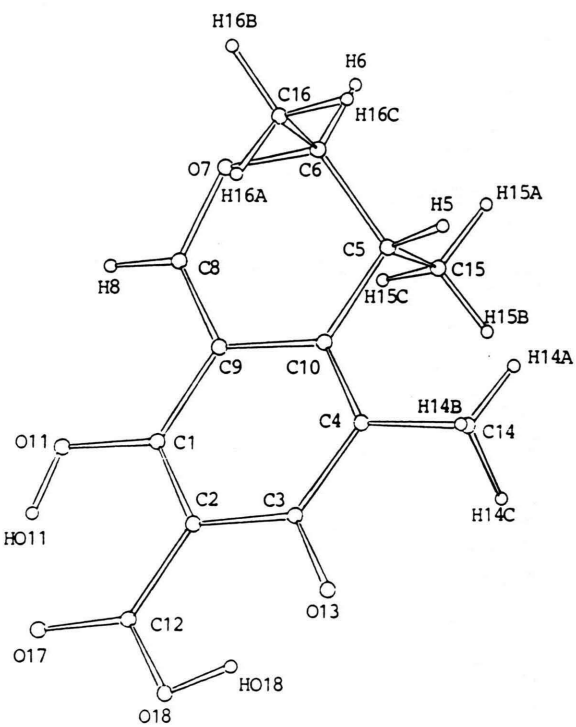

Fig. 1. Atomic numbering scheme for citrinin.

* Presented at the Sagamore X Conference on Charge, Spin and Momentum Densities, Konstanz, Fed. Rep. of Germany, September 1–7, 1991.

Reprint requests to Prof. R. Destro, Dipartimento di Chimica Fisica ed Elettrochimica, Università degli Studi di Milano, Via Golgi 19, I-20133 Milano, Italia.

0932-0784 / 93 / 0100-0099 $ 01.30/0. – Please order a reprint rather than making your own copy.

this paper we present the preliminary results of a study of the charge density and of the electrostatic properties of the *para* tautomer, based on a multipole analysis of a new set of diffraction intensities measured at 18–20 K.

Table 1. Cell parameters and space group of citrinin, $C_{13}H_{14}O_5$.

	290 K	18–20 K
a (Å)	13.439 (3)	13.257 (3)
b (Å)	7.289 (2)	7.239 (1)
c (Å)	12.234 (4)	12.131 (3)
V (Å^3)	1198	1164
Space group	$P2_12_12_1$	

The 20 K Data: Experiment and Calculations

Crystal data for citrinin are reported in Table 1. A total of about 37,000 diffracted intensities for the $h\,k\,l$ (18 K), $h\,\bar{k}\,l$ (20 K), $\bar{h}\,k\,l$ (17.5 K), and $\bar{h}\,\bar{k}\,l$ (17.5 K) reflections have been measured, with warming to room temperature after collection of each set of data. Only the first two sets ($h\,k\,l$ and $h\,\bar{k}\,l$) have been employed to yield the preliminary results presented here. Details of the data collection are listed in Table 2. The full treatment of all data, including profile analysis for the evaluation of the too-often ignored scan-truncation errors [3, 4], is under way.

Table 2. Data collection.

Diffractometer	Syntex $P\bar{1}$ equipped with the Samson Cryostat [13]	
Radiation	MoKα (graphite monochromated)	
Radius of crystal (mm)	0.18 (spherical)	
$(2\vartheta)_{max}$ (deg.)	108	
Temperature (K)	20 (1)	
Scan range (2ϑ, deg.)	$2.4+S_{\alpha1-\alpha2}$	
Scan rate (°/min) (2ϑ)	3	
No. of reflections	total measured	18 638
	independent	7 953
	with $I>0$	7 792
$(\sin\vartheta/\lambda)_{max}$	1.14 ($2\vartheta_{\alpha1}=108°$)	

Data not yet corrected for scan-truncation losses

Multipole (pseudoatom) analysis of the diffracted intensities, following the formalism developed by Stewart [5], and employing the VALRAY set of programs [6], has been essentially similar to the one we have employed in our previous studies of L-alanine [7, 8] and biscarbonyl[14]annulene [9, 10]. The parameters refined in the least-squares procedure included the atomic coordinates, the thermal parameters and electron population coefficients up to the octupole level for C and O atoms, while for H atoms only an isotropic thermal parameter and electron population coefficients up to the dipole level were allowed to vary in the calculations. The positional parameters for the H atoms were obtained in a previous refinement following the same procedure adopted for L-alanine [7]. A summary of the agreement factors for the multipole and the standard spherical-atom refinements are reported in Table 3.

Table 3. Refinement of X-ray diffraction data at 20 K.

	Spherical atom model	Multipole model
No. of data (N)	7792	7792
No. of parameters (P)	220	521
R (F)	0.063	0.051
wR (F)	0.038	0.020
R (F^2)	0.065	0.036
wR (F^2)	0.075	0.038
Goodness of fit	1.87	1.04

Results

Some relevant features of the derived electrostatic properties (electrostatic potential, molecular dipole moment, and Electric Field Gradients at the oxygen nuclei) are presented in the Figs. 2–5 and in the Tables 4–5.

The experimental, total charge density ϱ of citrinin and its Laplacian $\nabla^2\varrho$ have been obtained as in the case of L-alanine [11]. The results of the topological analysis of the experimental ϱ, as summarized by the properties of its bond critical points, are presented in Tables 6 and 7. A thorough comparison of the experimental vs. theoretical topological properties of the charge density distribution, of the type we have performed for L-alanine [12], is in progress.

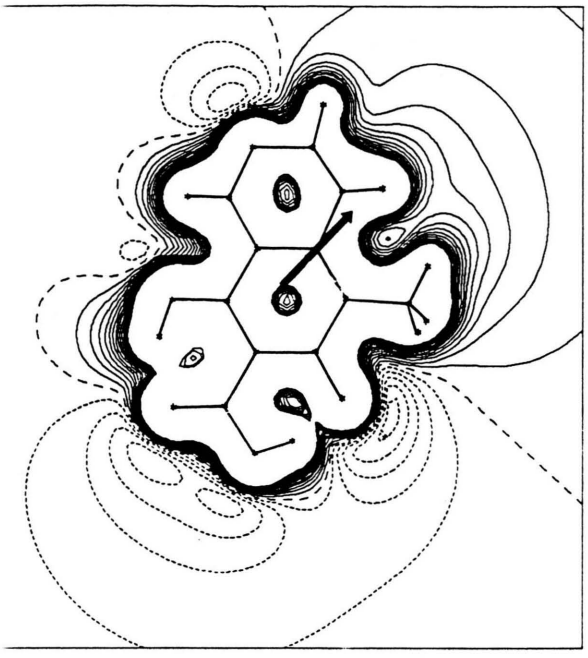

Fig. 2. Map (15 Å by 15 Å) of the electrostatic potential of citrinin (for a molecule "extracted" from the crystal), calculated in the plane defined by the atoms C1, C2, and C3. Atoms within ±1.0 Å from the plane are indicated by an asterisk. Contour levels are at an interval of 0.02 eÅ^{-1}, the maximum level plotted is 0.3 and the minimum is −0.1 eÅ^{-1}; solid lines positive, short dashed lines negative, large dashed lines zero contour. The minimum value of the electrostatic potential in the map is −0.108 eÅ^{-1} and occurs at ~1.2 Å from the atom O13. The direction of the molecular dipole moment is indicated by the arrow originating at the molecular centre of mass.

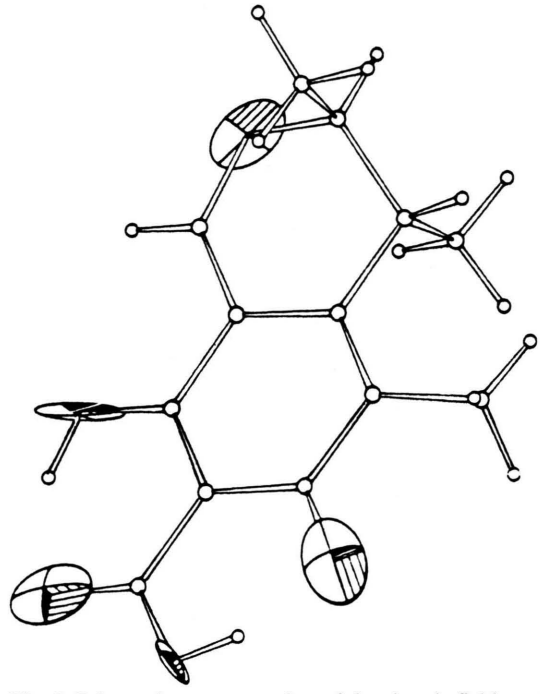

Fig. 3. Schematic representation of the electric field gradient (EFG) tensors at the oxygen atoms of citrinin. The lengths of the axes of the ellipsoids are proportional to the corresponding principal values $|V_{\alpha\alpha}|$, shifted to make all three values positive.

Table 5. Quadrupole coupling constants (QCC) and asymmetry parameters (η) for the oxygen atoms of citrinin.

Atom	QCC[a] (MHz)	η [b]
O7	−7.9 (6)	1.0 (1)
O11	−8.3 (6)	0.8 (1)
O13	−9.4 (7)	0.2 (1)
O17	−8.6 (7)	0.4 (1)
O18	−5.3 (7)	0.5 (2)

[a] The quadrupole coupling constant QCC = e^2qQ/h was evaluated assuming $eq = V_{zz}$.

[b] η is a measure of the deviation of the EFG tensor from axial symmetry and is defined as $\eta = (V_{xx} - V_{yy})/V_{zz}$, where V_{xx}, V_{yy} and V_{zz} are the principal components of the EFG tensor with the coordinate convention $|V_{zz}| \geq |V_{yy}| \geq |V_{xx}|$, fulfilling the trace relationship $\Delta V = V_{xx} + V_{yy} + V_{zz} = 0$.

Table 4. Molecular dipole moment $|\mu|$ (D) as derived from multipole analysis of the X-ray data [a].

Components	
μ_x	−6 (2)
μ_y	−1 (1)
μ_z	−4 (2)
Total $\|\mu\|$	7 (2) [b]

[a] The value of $|\boldsymbol{\mu}|$ from diffraction data is derived from pseudoatom monopole and dipole population parameters according to

$$\boldsymbol{\mu} = \sum [D_i^{\text{local}} \boldsymbol{d}_i - e \Delta P_i \boldsymbol{R}_i] ,$$

where the components of each vector d_i are the dipole population parameters and ΔP_i is the difference between the experimental monopole population parameter $P_i = P_{\text{core}} + P_{\text{valence}}$ and the nuclear charge Z_i. D_i^{local} is the expectation value

$$D_i^{\text{local}} = (e/3) \int_0^\infty R_d(r)\, r^3 \, dr$$

with $R_d(r)$ the radial function of the dipolar terms of the pseudoatom.

[b] The esd of $|\boldsymbol{\mu}|$ is calculated with respect to the molecular centre-of-mass as origin.

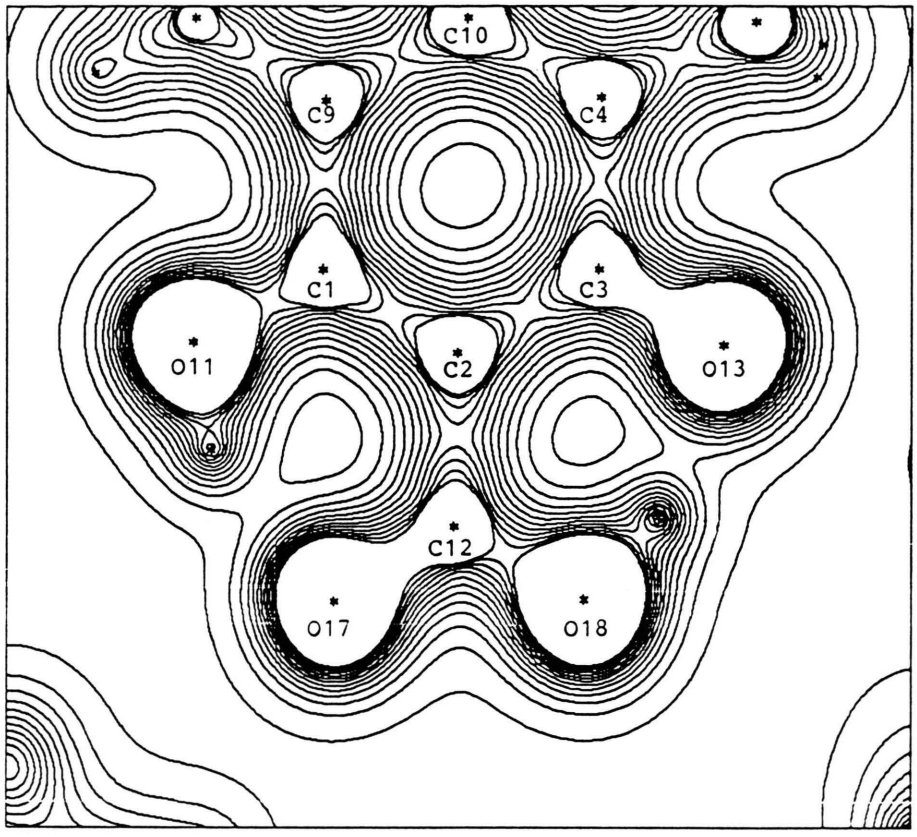

Fig. 4. Map (8 Å by 7 Å) of the total electron density ϱ of citrinin in the crystal, calculated in the plane parallel to the one defined by the atoms C1, C3, and C10 and displaced by 0.02 Å. Atoms within ± 1.0 Å from the plane are indicated by an asterisk. Contour levels are at an interval of 0.2 eÅ^{-3}, from a minimum value of 0.1 eÅ^{-3} to a maximum value of 2.5 eÅ^{-3}.

Table 6. Bond critical point properties over a crystal (intermolecular bonds).

Bond (a–b)	R (Å)	R_x (Å) [b]	ϱ_b	$\nabla^2\varrho_b$	λ_1	λ_2	λ_3	ε [c]
C1–C2	1.390	0.720	2.22	−20.80	−19.97	−13.64	12.82	0.46
C4–C10	1.364	0.675	2.25	−19.75	−20.09	−12.81	13.15	0.57
C8–C9	1.374	0.717	2.24	−19.70	−19.38	−13.46	13.14	0.44
C1–C9	1.436	0.756	2.08	−18.10	−17.06	−14.16	13.13	0.21
C2–C3	1.443	0.714	1.97	−15.07	−16.00	−12.47	13.40	0.28
C2–C12	1.470	0.697	1.84	−13.27	−14.62	−11.61	12.96	0.26
C3–C4	1.457	0.756	1.92	−14.96	−15.53	−12.41	12.99	0.25
C9–C10	1.448	0.735	1.91	−14.03	−14.73	−12.48	13.18	0.18
C4–C14	1.500	0.761	1.75	−12.27	−12.92	−12.03	12.68	0.07
C5–C6	1.522	0.739	1.69	− 9.47	−11.80	−11.33	13.65	0.04
C5–C10	1.509	0.746	1.70	−10.21	−12.03	−11.13	12.95	0.08
C5–C15	1.533	0.782	1.62	− 8.52	−11.14	−10.36	12.99	0.08
C6–C16	1.511	0.750	1.78	−11.80	−12.78	−12.25	13.23	0.04
C3–O13	1.268	0.554	2.79	−27.23	−27.85	−21.29	21.92	0.31
C12–O17	1.242	0.510	2.98	−39.07	−31.05	−25.86	17.84	0.20

Table 6 continues on p. 103.

Table 6. Bond critical point properties over a crystal (intermolecular bonds), continued from p. 102.

Bond (a–b)	R (Å)	R_x (Å) [b]	ϱ_b	$\nabla^2\varrho_b$	λ_1	λ_2	λ_3	ε [c]
C1–O11	1.321	0.566	2.43	−23.92	−23.38	−19.53	18.99	0.20
C6–O7	1.476	0.627	1.60	− 6.52	−11.76	−10.63	11.87	0.11
C8–O7	1.317	0.539	2.30	−22.14	−20.11	−18.19	16.15	0.11
C12–O18	1.311	0.521	2.39	−28.29	−24.58	−18.28	14.57	0.35
O17...HO11	1.691	1.087	0.35	4.44	−2.12	−1.94	8.51	0.09
O13...HO18	1.561	1.020	0.54	4.74	−3.55	−3.39	11.68	0.05

[a] ϱ in eÅ^{-3} and $\nabla^2\varrho$, λ_i (principal curvatures of ϱ at the critical point) in eÅ^{-5}, respectively. [b] Bond critical point distance to atom a. [c] ε is the bond ellipticity defined as $\varepsilon = \lambda_1/\lambda_2 - 1$.

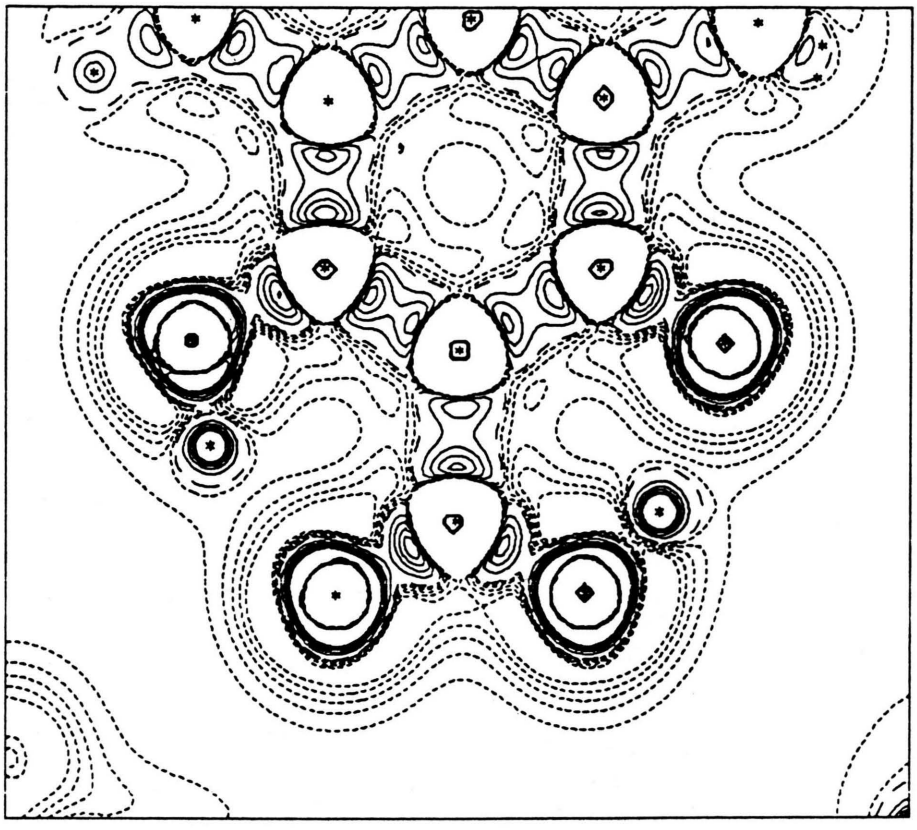

Fig. 5. Contour map (8 Å by 7 Å) of the Laplacian, $\nabla^2\varrho$, of the experimental electron density in the plane parallel to the one defined by the atoms C1, C3, and C10 and displaced by 0.02 Å. Atoms within ±1.0 Å are indicated by an asterisk. The large dashed lines are for zero level, the short dashed lines describe the positive region of $\nabla^2\varrho$, from 2 to 10 eÅ^{-5}, at an interval of 2 units. Negative values of the Laplacian, indicating charge concentration, are denoted by solid lines, ranging from 10 to 50 eÅ^{-5} at steps of 10 units.

Table 7. Ring critical point properties over a crystal. Units as in Table 6.

Ring	ϱ_b	$\nabla^2\varrho_b$	λ_1	λ_2	λ_3
C1–C2–C3–C4–C9–C10 (R1)	0.19	2.48	−0.38	1.28	1.58
C5–C6–O7–C8–C9–C10 (R2)	0.22	2.71	−0.54	1.55	1.69
C1–C2–C12–O17–HO11–O11 (R3)	0.19	2.60	−0.55	1.27	1.88
C2–C3–O13–HO18–O18–C12 (R4)	0.22	2.85	−0.65	1.43	2.08

[1] R. Destro and R. E. Marsh, J. Amer. Chem. Soc. **106,** 7269 (1984).
[2] R. Destro, Chem. Phys. Letters **181,** 232 (1991).
[3] R. Destro and R. E. Marsh, Acta Cryst. A **43,** 711 (1987).
[4] R. Destro, Aust. J. Phys. **41,** 503 (1988).
[5] R. F. Stewart, Acta Cryst. A 32, 565 (1976).
[6] R. F. Stewart and M. A. Spackman, VALRAY User's Manual, Dept. of Chemistry, Carnegie-Mellon University, Pittsburgh 1983.
[7] R. Destro, R. E. Marsh, and R. Bianchi, J. Phys. Chem. **92,** 966 (1988).
[8] R. Destro, R. Bianchi, and G. Morosi, J. Phys. Chem. **93,** 4447 (1989).
[9] R. Bianchi, R. Destro, and F. Merati, Collected Abstracts of the XII. Eur. Cryst. Meeting, Vol. 3, p. 404, USSR Academy of Sciences, Moscow 1989.
[10] R. Bianchi, R. Destro, and F. Merati, in: The Application of Charge Density Research to Chemistry and Drug Design (G. A. Jeffrey and J. F. Piniella, eds.), Plenum Press, New York 1991.
[11] R. Destro, R. Bianchi, C. Gatti, and F. Merati, Chem. Phys. Letters **186,** 47 (1991).
[12] C. Gatti, R. Bianchi, R. Destro, and F. Merati, J. Mol. Struct. (Theochem) **255,** 409 (1992).
[13] S. Samson, E. Goldish, and C. J. Dick, J. Appl. Crystallogr. **13,** 425 (1980).